

Innate immune response and distinct metabolomic signatures together drive and shape the SARS-CoV-2-specific T cell response during COVID-19

Akshay Binayke¹, Aymaan Zaheer^{2†}, Jyotsna Dandotiya^{1†}, Sonu K Gupta³, Shailendra Mani³, Manas Tripathi², Upasna Madan¹, Tripti Shrivastava³, Yashwant Kumar³, Anil K Pandey⁴, Deepak K Rathore³, Amit Awasthi^{1,2*}

¹Immunobiology Lab, Translational Health Science and Technology Institute, Faridabad, India;

²Immunology Core, Translational Health Science and Technology Institute, Faridabad, India;

³Translational Health Science and Technology Institute, Faridabad, India;

⁴ESIC Medical College and Hospital, Faridabad, India.

*Corresponding author. Email: aawasthi@thsti.res.in

† Equal Contribution

Abstract:

The underlying factors contributing to the evolution of SARS-CoV-2-specific T cell response during COVID-19 infection remain unidentified. To address this, we characterized innate and adaptive immune responses with metabolomic profiling longitudinally at three different time points (0-4, 7-9, and 14-16 days post-COVID-19 positivity) from young mildly symptomatic active COVID-19 patients who got infected with ancestral virus. We observed the induction of anti-RBD and SARS-CoV-2 neutralizing antibodies together with antigen-specific T cell responses as early as 0-4 days post-infection. T cell responses were largely preserved against the delta and omicron variants as compared to the ancestral strain. We determined innate immune responses at an early (days 0-4 post-COVID-19 positivity) time point of active infection in response to TLR 3/7/8 mediated activation. Interestingly, the innate immune response exhibited by the elevated levels of IL-6, IL-1 β , and IL-23 correlated with a robust SARS-CoV-2-specific Th1 response at the later time point (14-16 days post covid positivity). To further understand the association of metabolic pathways induced upon active COVID-19 infection with innate and T cell response, metabolomic profiling was performed. As compared to healthy individuals, COVID-19 patients displayed a distinct metabolic signature with an enrichment of pyroglutamate, itaconate, and azelaic acid, which correlated with the SARS-CoV-2-induced innate and T cells response. Our observations reveal mechanisms and potential interventional approaches that may assist in COVID-19 therapeutics and vaccine adjuvant strategies.

One Sentence Summary: T cell Immune response against SARS-CoV-2 is driven by a proinflammatory innate immune response and an associated metabolic signature in young adults.

INTRODUCTION

While significant efforts have been made to understand the immune-mediated clearance of the SARS-CoV-2 infection (1), the contribution of metabolites together with innate cytokines in the evolution of the SARS-CoV-2-specific T cell response is not clearly understood. Anti-SARS-CoV-2 antibodies are critical in minimizing the spread of the virus. However, the cross-reactivity of neutralizing antibodies against SARS-CoV-2 VOCs remains poor. Moreover, they dissipate rapidly over 4-6 six months from convalescent and vaccinated individuals (2). In this case, T cells become crucial in preventing severe COVID-19 from SARS-CoV-2 and its VOCs. Although emerging VOCs acquire multiple mutations to evade the immune response generated either through natural or vaccination derived immunity, most T cell epitopes remain conserved and unaffected by mutations (3). Importantly, SARS-CoV-2 memory T cells persist for a long time and thus provide protection upon reinfection of the SARS-CoV-2 and its emerging VOCs (4). The frequency and magnitude of antigen-specific memory T cells could potentially affect the clinical manifestations of the disease. Therefore, understanding the factors that shape the magnitude and breadth of the T cells response during SARS-CoV-2 infections has become even more significant.

Correlates of protection against SARS-CoV-2 ranging from innate to adaptive immune responses have been identified (5). CD4⁺ and CD8⁺ T-cell activation was found to be inversely correlated with the disease severity and death (6). In contrast, non-Th1 cytokines (IL-4, IL-5, and IL-10) were found to be associated with respiratory failure in COVID-19 patients (7), implying that a robust Th1-biased response is essential in mediating recovery from COVID-19. Studies highlighted the significance of the antibody response, particularly the IgG response against the Receptor Binding Domain (RBD) correlating with patient survival (8). Moreover, a coordinated B and T cell response, especially anti-spike/anti-RBD IgG together with IL-2/IFN- γ secreting activated CD4⁺ and Granzyme B/TNF- α expressing CD8⁺ T-cells, were

implicated in successful viral clearance (9). Although an orchestrated adaptive immune response is imperative for mild disease, role of innate cytokines in generating a robust T cell response is not clearly understood in COVID-19. Systems biology studies suggest that proinflammatory cytokines, IL-6, IL-1 β , and TNF- α , originate from the lung tissue and not from the peripheral blood cells in severe COVID-19 patients (10), further emphasizing the role of innate immune response in shaping the SARS-CoV-2-specific T cell response. Nonetheless, a precise mechanism by which the initial steps of innate immune activation lead to shape T cell response in SARS-CoV-2 infections and how this mechanism is subverted in severe cases has not yet emerged. Understanding the generation of the systemic immune response during COVID-19 will enable research into therapies and vaccinations that induce strong innate, humoral, and cellular responses against a pathogen. It could also inform better diagnostic methods for clinicians to predict outcomes based on patient immunophenotype.

Viral nucleic acid recognition by Toll-Like Receptors (TLRs) on innate immune cells is essential for initiating an appropriate immune response to viral infection. While TLR-7/8 recognizes ssRNA of SARS-CoV-2 and induces IL-6, IFN- α , TNF α , and type 1 interferon, TLR3 recognizes dsRNA, a replication intermediate in SARS-CoV-2, and activates antiviral response (11). TLR signaling could be vital in initiating an innate immune reaction to SARS-CoV-2 and subsequently inducing a robust T cell response. We used TLR 3, 7, and 8 agonists to stimulate PBMCs from COVID-19 patients, examining their phenotypes in response to the SARS-CoV-2 spike protein to understand how TLR-mediated signaling affects immunity against COVID-19.

Innate immune responses are modulated by metabolic pathways that provide the metabolites and energy necessary for shaping T cell response. COVID-19 patients were found to have altered metabolic pathways and dysregulation of energy production. Exploring the metabolic landscape during active COVID-19 could complement an understanding of the phenotypic

changes in those individuals during infection, providing potential pathways to target for therapeutically modulating the immune response for COVID-19 patients (12). Additionally, key immunomodulatory metabolites in COVID-19 disorder could be provided to immunocompromised patients as supplements to stimulate appropriate immune responses.

Here, we examine innate and adaptive immune responses at early and later time points of infection and try to establish the relationship between these stages of the immune response in mild cases where the virus was successfully cleared. We aim to shed light on the coordination of the innate and adaptive immune responses over the course of acute COVID-19 and understand the phenotypes of the immune cells involved at each stage to gain a holistic understanding of how different branches of the immune system act sequentially during infection. This will aid in creating a general overview of the immune response to COVID-19 infection. Longitudinal metabolic analysis of COVID-19 patients in concurrence with the immune phenotype may point out distinct metabolites that significantly correlate with the innate and adaptive immune responses. Our results reveal that the antiviral TLR specific proinflammatory cytokine activity by PBMCs may be beneficial in generating a robust immune response against COVID-19 infection.

RESULTS

Antibody response against RBD protein of ancestral SARS-CoV-2 and VOCs

To study the kinetics of the immune response against the SARS-CoV-2, we first investigated the IgG response against the SARS-CoV-2 RBD protein using Enzyme-linked immunosorbent assays (ELISAs). For all assays, blank-subtracted colorimetric values were normalized to a pre-pandemic negative control plasma sample added to each assay plate and expressed as ratios to this pool of negative samples as described previously (13). We found seropositivity (above cut-off) in 66% (14/21) patients as early as visit 1 of the positive report (**Fig. 1B**), which increased significantly to 85% such that the median IgG response increased three-fold by V2 and V3. When we tested the antibody response against the RBD proteins of the delta (B.1.617.2) (**Fig. 1C**), beta (B.1.315) (**Fig. 1D**), and alpha variants (B.1.1.7) (**Fig. 1E**), the seropositivity ratio was significantly reduced. Similarly, the neutralizing antibodies (NAb) could be detected as early as Day 0-4 of COVID-19 positivity in about 48% (10/21) of the samples, and the median NAb titers increased significantly by V2 and V3 (**Fig. 1F**). As reported previously (14), we also observed a sharp decline in the NAb titers against the delta variant compared to the ancestral virus ($p < 0.0001$, Fig. 1H). We observed that even by V3, only 33% (7/21) individuals had detectable levels of NAb against the Delta variant (**Fig. 1G**), therefore suggesting that the humoral immune protection against VoCs in recently infected individuals is broadly inadequate.

Early induction of antigen-specific T cell response in COVID-19 patients

We studied the initiation of the antigen-specific T cell response from the PBMCs of active COVID-19 patients by stimulating them with peptide pools spanning the entire length of the spike protein for 20-24h. The T cell response was measured by calculating the expression of T cell receptor (TCR)-dependent activation-induced markers (AIM) (9) and Th1 cytokine using

live-cell flow cytometry (15). The CD4⁺ T cells co-expressing CD137 and OX-40 are designated as CD4⁺AIM⁺ cells (**Fig. 2A**), and the CD8⁺ T cells co-expressing CD137 and CD69 are defined as CD8⁺AIM⁺ cells (**Fig. 2D**) (9, 16).

With the progression of time since the detection of SARS-CoV-2 infection, we found a significant increase in the antigen-specific T cell response. The AIM⁺ CD4⁺ T cells could be observed as early as visit 1 (6/21), which may be attributed to pre-existing cross-reactive T cells from prior common cold coronavirus infections (17). The magnitude and extent of SARS-CoV-2 specific CD4⁺ T cells increased significantly by visit 2 (day 7, $p = 0.0027$) and by visit 3 (day 14, $p = 0.0028$) (**Fig. 2 A-B**). Similar to the previous reports (9), the AIM⁺ CD4⁺ T cells were observed in ~76% of the patients by visit 3 (16/21). Likewise, AIM⁺ spike-specific CD8⁺ T cells were detected as early as visit 1 (4/21). Interestingly, the frequency and magnitude of AIM⁺ CD8⁺ T cells peaked quickly by visit 2 ($p = 0.021$) and did not change significantly by visit 3 ($p = 0.52$) (**Fig. 2 C-D**). Notably, antigen-specific CD8⁺ T cells were detected in only 57% (12/21) of the patients, consistent with the previous findings reported by Moderbacher et al., 2020 (9).

The spike peptide pool stimulated PBMCs were also tested for intracellular expression of cytokines such as IFN γ , IL-2, IL-9, IL-17, and Perforin (**Fig. 2 G, J**). We observed a predominantly Th1 skewed CD4⁺ T cell response with intracellular IFN gamma expression significantly increasing from V1 to V3 ($p=0.014$, **Fig. 2H**). The median CD4⁺IL-2⁺ T cells also increased with time; however, the difference was non-significant ($p= 0.268$, **Fig. 2I**). The CD8⁺ T cell response was evaluated by the intracellular expression of IFN γ and Perforins. Similar to the intracellular CD4⁺ T cell response, the functional SARS-CoV-2 specific cytotoxic T cell frequency significantly increased by visit 3 (**Fig. 2 K, L**). Therefore, to summarize, we found a steady increase in the CD4 and CD8 AIM and functional T cell

response that was predominated by intracytoplasmic expression of IFN- γ in both CD4+ and CD8+ T cells.

The culture supernatant was collected to further understand the range of cytokines released after stimulation of PBMCs with peptide pool. The release of cytokines after 18-20h of stimulation was calculated by cytokine bead assay. With the progression of time, we observed a steady increase in the secretion of Th1 specific cytokines such as IFN- γ (mean: V1:100 pg/ml; V2: 810 pg/ml; V3: 1352 pg/ml , **Fig. 3A**), TNF α (mean: V1: 134 pg/ml; V2: 206 pg/ml; V3: 478 pg/ml, **Fig. 3B**), and IL-2 (mean: V1: 196 pg/ml; V2: 432 pg/ml; V3: 429 pg/ml, **Fig. 3C**) whereas Th-2 and Th-17 specific cytokines did not change significantly (**Fig. 3 D, E, G**). The cytotoxic response, evaluated by the expression of Granzyme B, increased extensively by 14 days after virus detection ($p=0.045$, mean V3= 841 pg/ml, Fig. I). Notably, as the antigen-specific T cell response increased, the proinflammatory cytokines IL-23 and IL-6 upon antigen exposure increased significantly by visit 3 (IL-6: mean:898 pg/ml; $p=0.013$; IL-23: mean: 711 pg/ml; $p=0.034$).

T cell response against VOCs is largely preserved in active COVID-19 patients

Since several variants of SARS-CoV-2 arise one after the other (14, 18), we wanted to test if the T cell response elicited by day 14 in active COVID-19 patients caused by the ancestral virus could cross-react with the delta and omicron spike protein. We shortlisted the dominant CD4 and CD8 T cell epitopes against the spike protein and found that 96% each of the dominant CD4 and CD8 epitopes are conserved against the delta spike, whereas 80% and 82% of CD4 and CD8 dominant epitopes, respectively, are conserved against the Omicron spike (Table S2). Next, we functionally tested the PBMCs of active COVID-19 patients from V2 and V3 ($n=24$) against the spike peptide pools of the ancestral, delta, and omicron variants (Fig. 4). We observed that the T cell response is largely conserved except in a few parameters, where the response against the omicron and delta spike is reduced by 1.3 to 1.5-fold, respectively.

Compared to the wildtype response, the geometric mean of AIM+ CD4+ response was reduced by 31% against delta ($p=0.0162$) and 58% against Omicron spike ($p=0.0005$) (**Fig. 4A**). However, the functional profile was broadly comparable among the variants (**Fig. 4 B-D**). We also did not find any significant differences between the functionality of the antigen-specific T cells as determined by the expression of intracellular cytokines such as IFN- γ , IL-2, and TNF α (**Fig. 4 E**). A pairwise comparison further revealed that the CD4 AIM response was preserved entirely in 30% of samples stimulated with delta spike peptides and 15% stimulated with the omicron spike peptides (**Fig. 4 F, G**).

The geometric mean antigen-specific CD8 AIM response was reduced by 3-5 fold in the delta and omicron variants (**Fig. 4 H**). However, the functional phenotypes of the antigen-specific CD8 T cells were similar among the VoCs compared to the wildtype (**Fig. 4 I-K**). The pairwise comparison further revealed a maximum reduction in 66% of individuals against the spike of delta variant and 75% against the spike of omicron variant (**Fig. 4 L, M**).

Taken together, although the humoral immune response is abrogated against the VoCs in actively infected individuals, the cellular immune responses persist. Our results imply the importance of the cellular immune responses against COVID-19 and therefore underline the need for further investigation to understand what processes determine the generation and function of a robust T cell response during active COVID-19.

Early proinflammatory innate immune response predicts robust T cell response

Next, we tested how innate immune response shapes adaptive immunity, especially T cells immune response in active COVID-19 patients, given the earlier findings that COVID-19 infection impairs pDCs and myeloid cells (10, 19). We performed *ex vivo* stimulation of Visit 1 PBMCs of our COVID-19 cohort with a cocktail of synthetic agonists of toll-like receptor (TLR) 7, TLR8 (TLR7/8), and TLR3, which are known to sense virus-derived molecules and

initiate an antiviral response (20). In the presence and absence of the TLR agonists cocktail of poly I:C (TLR3) and R848 (TLR 7/8), the PBMCs were cultured for 24h as described previously (10). The cytokine level of IL-1 β , IL-6, IFN- γ , CCL2, IL-8, IL-10, IL-12p70, IL-18, IL-23, IL-33, and TNF α in the culture supernatant was evaluated by a magnetic bead-based cytokine assay. The cytokines levels in TLR stimulated wells were significantly higher than in the unstimulated wells (**Fig. S2**). Therefore, to account for the differences in the number of PBMCs cultured, fold change in the cytokine response was evaluated by dividing the cytokine response in stimulated wells by unstimulated wells. The fold change in TLR stimulated samples was compared with the fold change in T cell response elicited in Visit 3 (day 14 since RT-PCR confirmed report) (**Fig. 5A**).

The intracellular cytokine levels were highly correlated with the cytokines in the culture supernatant, indicating the robustness of the sample analysis (**Fig. 5 A**). For example, the CD4+ and CD8+ T cell IFN- γ significantly correlated with the IFN- γ levels in the culture supernatant (CD4: $r = 0.921$, $p = 3.10 \times 10^{-9}$; CD8: $r = 0.728$, $p = 1.81 \times 10^{-4}$; **Fig. 5A**). The Pearson correlation analysis showed that the PBMCs from individuals that exhibit a heightened proinflammatory innate immune response during the early time points of infection (Visit 1) possessed a broader and stronger T cell immune response during the later time point of infection (Visit 3). Proinflammatory cytokines such as IL-6, IL-1 β , and IL-23 upon TLR stimulation correlated significantly with the spike-specific T cell immune response in the form of the secretion of IFN- γ , TNF α , and Granzyme B (GZB) (**Fig. 5B**). Surprisingly, the Th17 differentiating cytokines, IL-6, IL-23, and IL-1 β , of innate immune cells displayed a signature of correlation with the magnitude of SARS-CoV-2-specific T cell response of the PBMCs from Visit 3. In contrast, the remaining cytokines such as IFN- γ , IL-12p70, CCL2, IL-10 predominantly did not display any correlation. Moreover, the proinflammatory cytokines did not correlate with other cytokines such as IL-5, IL-17 but correlated with the IL-4 cytokine release (**Fig. 5B**).

Metabolomic alterations in active COVID-19

The correlation between metabolic profile with innate and adaptive T cell response in active COVID-19 infection remains unexplored. Moreover, altered metabolites in active COVID-19 patients might help predict the disease outcome and anti-SARS-CoV-2 immune responses. To determine the metabolic landscape in active COVID-19 patients, we performed a plasma metabolomic analysis to identify changes throughout COVID-19 infection. Multiple reports have identified metabolomic alterations during COVID-19 (21-24). To obtain a broad view of the metabolic status, we studied the longitudinal plasma metabolite profile in our cohort of 21 COVID-19 patients and compared them with the plasma of 12 healthy volunteers (Table S1). The plasma samples from visit 1 and visit 3 were processed for UHPLC-MS/MS analysis, and 240 different metabolites were identified. These 240 metabolites were further screened to remove drugs and other artificial compounds and derivatives to obtain 176 metabolites. Unsupervised PCA analysis of the metabolites in our patient cohort displayed a clear distinction that separated the control (healthy individuals), COVID-19 early time point (V1), and late time point (V3) individuals (**Fig. 6A**). The Partial Least Squares – Discriminant Analysis (PLS-DA) was employed to identify the top-15 important metabolites across the three different groups (**Fig. 6 B**). Moreover, hierarchical clustering of top 50 metabolites showed a notable shift in the metabolic signature among acute COVID-19 patients compared to the healthy individuals (**Fig. 6 C**). The PLS-DA and hierarchical clustering analysis pointed out that the levels of metabolites and derivatives of the Citric Acid cycle, such as Citrate, Itaconate, and trans-aconitate, were significantly reduced in COVID-19 patients. In contrast, metabolites such as glutamic acid derivatives – Pyroglutamate, N-methyl-L-glutamic acid were enriched in the plasma of COVID-19 patients. Of the 176 metabolites, 158 were significantly differentiated in COVID-19 patients (FDR<0.001), exhibiting a distinct metabolic profile. Pathway enrichment analysis using the KEGG database showed that the metabolites involved in the Phenylalanine

metabolism; Arginine and Proline metabolism, Alanine, aspartic acid, and glutamate metabolism, were significantly altered during COVID-19 (**Fig. 6 E**). While comparing the metabolic profile during the early and later stages of infection, 33 metabolites were significantly down and 13 significantly up ($p=0.001$, $FC>1.5$, **Fig. 6 D**).

To understand the immune-metabolomic interaction, we performed a Pearson correlation of metabolites with the innate and adaptive immune responses in COVID-19 patients and shortlisted the significantly correlating metabolites ($r>0.5$, $p<0.05$). Pathway analysis of plasma metabolites that significantly correlated with the innate immune response from V1 and the T cell immune response from V3 samples showed that the metabolites involved in arginine biosynthesis, histidine metabolism, alanine-aspartate, and glutamate metabolism were enriched in plasma samples from V1 as well as V3 (**Fig. 7 A-B**). Metabolites such as norvaline, urea, and azelaic acid were highlighted based on the VIP score of the individual metabolites, which increases drastically during COVID-19 (**Fig. 7 F-I, M, Fig. S4**). Notably, the metabolites such as pyroglutamate, itaconate, and norvaline which are involved in the glutathione metabolism, citrate cycle, and amino acid biosynthesis, correlated significantly with the early and late-stage immune responses (**Fig. 7**).

DISCUSSION

The COVID-19 pandemic is continuing, as new waves are driven by emerging variants (25). It is, however, essential to understand the interplay between innate immune responses and metabolic landscape shaping long-lasting SARS-CoV-2-specific T cell responses. This study longitudinally investigated antibody and T cell response during acute infection and integrated them with the early-stage antiviral innate immune response and metabolomic signature.

Although there are reports that longitudinally studied the patient metabolomic signature (26) and single-cell transcriptomic landscape in COVID-19 patients (35), no study correlated the functional innate and T cell response with the metabolic landscape. Our literature survey did not find any study comparing the T cell immune response in COVID-19 active patients against the spike proteins of ancestral, delta, and omicron variants. In this study, the samples were collected during the first wave of COVID-19 before the existence of delta, and omicron VoCs, which allowed us to determine how T cells primed with the ancestral stain react with spike antigen of delta and omicron together with the correlation with innate immune response and metabolomic changes.

To study the humoral immune response, we first tested the IgG response against the RBD proteins of WT and VoCs. Consistent with the previous reports from convalescent samples of COVID-19 (27), we observed a sharp decline in the cross-reactivity of RBD-specific IgG and neutralizing antibodies against VoCs in active COVID-19 patients.

The antigen-specific T cell response was evaluated by the expression of the activation-induced markers, intracellular cytokine expression, and secretion upon spike peptide pool stimulation. In this way, we attempted to acquire the breadth and magnitude of T cell response during active COVID-19. We found that the frequency of activated induced marker (AIM) in CD4⁺ and CD8⁺ T cells was consistent as reported previously (9). Th1 skewed response is one of the

signatures of anti-SARS-CoV-2 T cell immunity. We observed that the early-stage T cells predominantly expressed IFN gamma, but not IL-2, as observed in vaccinated and convalescent individuals (4, 9, 15). Moreover, unlike IFN γ , IL-2 expression did not increase with the progression of days from the COVID-19 positivity report, suggesting that the IL-2 is not primarily involved in the early T cell response and is possibly dominant in the later stage of SARS-CoV-2 infection.

We observed that the T cell response elicited during the active infection persists but is relatively reduced against the delta and omicron compared to the wild type. The extent of reduction in the magnitude of T cell response against VoCs is more prominent in our cohort than previous reports in vaccinated individuals (28). Since the samples were collected during acute infection, the overall magnitude of T cell response is low in acute samples (4) and therefore may result in a limited scope for cross-reactivity against the VoCs.

Increased plasma IL-6, TNF-a and IL-1b are characteristics of severe COVID-19 patients (29). However, it has now been well established that the source of these proinflammatory cytokines is not the innate immune cells but the non-immune host tissues such as lungs (10). Furthermore, in severe COVID-19, the innate cell expression of these proinflammatory cytokines is rather significantly reduced (10). Our investigation of innate and T cell response across the early stages of infection showed that the PBMCs from individuals with a strong proinflammatory innate immune response also exhibit a robust T cell response against SARS-CoV-2. The correlation of proinflammatory Th17 differentiating cytokines, IL-23, IL-1b, and IL-6, with the Th1 response in the later stages of disease needs further investigation. Interestingly, we recently reported that IL-17 transcripts were higher at the early stage of SARS-CoV-2 infection in hamsters (30). Therefore, it may be interesting to investigate further if there is any Th1/Th17 plasticity that may play a role in the development of T cell response during COVID-19

infection. Such investigations are fundamental for designing adjuvants that trigger a robust and long-lasting memory T cell immunity.

There is an orchestrated symphony between the metabolism and immune responses where both players harmonize (31). We investigated how the metabolic state modulates the immune response and vice versa by performing the plasma metabolomic analysis of the COVID-19 patients. Based on our analysis, we found that there was a significant correlation between the arginine biosynthesis metabolites and the SARS-CoV-2 specific immune responses. L-Arginine is an immunomodulatory metabolite that plays a critical role in the pathways involving inflammation, immune regulation, and via its metabolism leading to the generation of nitric oxide (NO), which plays an intrinsic role in Th cell activation and differentiation (32). Notably, metabolites involved in arginine biosynthesis have been reported to be significantly altered in severe COVID-19 patients (26). We also found a significant increase in Norvaline during COVID-19 (**Fig. 6C**), and the levels of norvaline correlated with the CD8+ T cell response (**Fig. 7F**). Conversely, norvaline is an arginase inhibitor (33), suggesting that arginine and norvaline may get involved in a corrective balancing of the immune response as described previously in animal studies (33).

Similar to the previous observations, itaconate, a known immunomodulatory metabolite, levels were significantly and distinctly reduced in the COVID-19 patients (**Fig. 6C**). Notably, the levels of itaconate were recovering in V3 (**Fig. 7N**). *In vitro* experiments have also established that itaconate suppresses the expression of IL-1 β and IL-6 (34). It was recently reported that itaconate mediates its effect by activating Nrf2 (35), which binds to the promoter region of proinflammatory cytokine genes and blocks transcription in macrophages (36). The correlation between the increasing levels of itaconate and the increasing levels of IFN-g during V3 may prove to be an important observation, where now that the T cell response is ready to take its

course against infection, the proinflammatory innate immune responses must be turned down to prevent the uncontrolled state of hyper inflammation observed in severe disease. Notably, it has been reported that itaconate levels are progressively reduced with COVID-19 disease severity (37). Furthermore, both citrate and aconitate were reduced in COVID-19 patients (Fig. 6C), thus signifying the importance of the itaconate and other citric acid cycle derivatives in the COVID-19 pathogenesis and immunomodulation. Azelaic acid was identified as one of the most important metabolites identifying COVID-19 patients (38). Azelaic acid is a tyrosinase inhibitor (39), and our analysis shows that the levels of azelaic acid correlate with the innate and adaptive immune responses against SARS-CoV-2 (**Fig. 7G-I**).

Our analysis underlines the importance of T cell response against the upcoming variants of SARS-CoV-2. We show how the PBMC derived innate immune responses are critical for generating a robust T cell response and how the metabolites are essential immunomodulatory aspects investigators should further look into.

Limitations of the Study:

Firstly, the sample size of COVID-19 patients was limited to 21 donors, and we observed lower levels of antigen-specific CD8⁺ T-cells likely due to the use of 15mer peptides. Secondly, we did not test the type I interferon levels upon TLR stimulation of PBMCs. Future studies may be employed to study further the correlation of type I interferon immunity with T cell responses. Furthermore, we did not evaluate the longevity of T cell immune responses in these patients. Finally, the active COVID-19 samples were collected from a relatively young, male-dominant cohort; further studies are therefore required to confirm if a similar phenotype is observed in older adults, children, and most importantly, among the vulnerable population.

MATERIALS AND METHODS

Study Design: To investigate the factors that contribute to the priming of a robust anti-SARS-CoV-2 T cell response, we longitudinally studied antibody and T cell immune responses at early time points of acute infection in young mildly symptomatic acute COVID-19 patients by collecting blood samples from RT-PCR positive COVID-19 patients on day 0-4 (indicated as "Visit 1 or V1"), day 7 (indicated as "Visit 2 or V2") and day 14 (indicated as "Visit 3 or V3") from the date of RT-PCR positive infection report. Clinically relevant medical information (e.g., age, patient-reported symptoms) was collected at the time of enrolment from the subject or the hospital medical records. For comparison, blood was also collected from age-matched SARS-CoV-2 RT-PCR negative healthy volunteers as a negative control group (**Table S1**). The clinical cohort was considerably young and consisted of 8 females and 13 males with a median age of 28 years (IQR: 25:34) (**Table S1**). From the collected blood samples, we separated the plasma and PBMCs, which were cryopreserved until further experimentation. The humoral immune response against SARS-COV-2 and its variants was evaluated using the plasma samples collected from the 21 patients. PBMCs from all three-time points were used to determine antigen-specific T cell response dynamics during acute COVID-19. To study the status of innate immunity against SARS-COV-2, we *ex vivo* stimulated the PBMCs of visit 1 samples with a cocktail of TLR 3/7/8 agonists, and the released cytokines were quantified. We performed a Pearson correlation analysis of the innate immune response from V1 samples and compared them with the SARS-CoV-2 specific T cell immune response of V3. The metabolic signature obtained from the plasma was further correlated with the SARS-CoV-2 specific innate and T cell immune responses (**Fig. 1A**).

Human Ethics: All the experiments were performed according to the suggested guidelines of the Institutional Ethics Committee (Human Research) of THSTI and ESIC Hospital, Faridabad

(Letter Ref No: THS 1.8.1/ (97) dated 07th July 2020). Human blood samples were collected from COVID-19 patients and healthy individuals after obtaining written informed consent. Individuals were enrolled in this study based on the inclusion/exclusion criteria prescribed by the Institutional Ethics Committee (Human Research) of THSTI.

THSTI In-house RBD IgG ELISA:

ELISAs to detect IgG binding to RBDs were performed as previously described (40) with some modifications. A positive convalescent and negative control sample were added to each plate at a single point concentration for normalization. The assay results were normalized by dividing the blank subtracted readings of each sample by negative control to obtain the fold change reading. Cut-off values were calculated with the following formula: Cut-off = Average fold change value of negative samples (pre-pandemic plasma samples) + 3* SD of fold change value of negative samples.

Virus Neutralization Assay:

Virus microneutralization assay titers were estimated as described previously (10). Briefly, plasma samples were serially diluted from 1/20 to 1/2560 and incubated with the wildtype and the delta SARS-CoV-2 isolates (suppl. methods). 50% neutralization values were estimated with four-parameter logistic regression.

Peptide Pool: 15mers peptide pools with an overlap of 11 amino acids spanning the entire sequence of Spike protein (157+158 peptides, JPT, PepMix, Cat. No.PM-WCPV-S-1 (Ancestral), PM-SARS2-SMUT06-1 (Delta) and PM-SARS2-SMUT08-1 (Omicron)) were used for the determining the WT, B.1.617.2 and B.1.1.529 SARS-CoV-2-spike specific T-cell responses by AIM assay, ICS and cytokine bead assay.

Evaluation of SARS-CoV-2 Specific T cell response: PBMCs were stimulated with peptide pools at a 2 µg/ml/peptide concentration and with an equimolar concentration of dimethyl sulfoxide (DMSO) as a negative control. Phytohemagglutinin (PHA, Roche; 5µg/ml) was used as a positive control. Any sample with a low PHA stimulation was removed from analysis for quality control. The cells were cultured for 22-24h, and monesin (GolgiStop™, BD Bioscience, USA) was added during the last six hours. After stimulation with peptides, the culture supernatant was separated and stored at <-20°C until further use, and the cells were stained for flow cytometry. Samples were acquired on a fluorescence-activated cell sorter (FACS) Symphony™ instrument (BD Biosciences) using BD FACSuite software version 1.0.6 and analyzed with FlowJo software version VX (FlowJo LLC, BD Biosciences). Functional profiles were deconvoluted by employing Boolean gating in FlowJo version XV followed by downstream representation using SPICE version 6.1 (<https://niaid.github.io/spice/>). Spike-specific cytokine production was background-subtracted by the values obtained with the DMSO-containing medium. Negative values were set to the Limit Of Detection (LOD). The stimulation index (SI) and LOD were calculated as described previously (41); briefly, the SI was calculated by dividing the frequency of AIM+ CD4 or CD8 cells recorded in stimulated wells by the unstimulated wells.

Metabolomic Analysis: Metabolomic profiling of plasma metabolites was performed as described previously (42, 43). Briefly, the data was acquired on an Orbitrap Fusion mass spectrometer (Thermo Scientific) coupled with the heated electrospray ion source. The mass resolution for MS1 acquisition was set at 120,000, whereas for MS2 mode, the mass resolution was 30,000. The mass range for data acquisition was 60–900 da. The extracted compounds were separated on a UPLC ultimate 3000 and the data was acquired on a HSS T3 and HILIC columns. The LC/MS obtained data were processed using the Progenesis QI for metabolomics (Nonlinear dynamics, a Waters Company) software using the default setting.

In vitro stimulation of PBMCs with TLR agonists:

PBMCs were stimulated as previously described (10), with some modifications. Approximately one million cells were added to each well, and all wells received stimulation with a viral cocktail containing 4.0 µg/ml R848 and 25 µg/ml poly I:C. Negative control DMSO stimulated cells were also cultured for each sample. The cells were incubated in a 5% CO₂ incubator at 37°C for 24 hours, after which supernatant was collected for analysis of cytokine secretion.

Analysis of Cytokine Secretion by Luminex:

Cytokine secretion in the cell culture supernatant was analyzed with a customized Premixed Multi-Analyte Luminex Discovery Assay kit (LXSAHM-10, R&D systems). The assays were performed as per the manufacturer's instructions. The analytes examined were Granzyme B, IL-2, IL-5, IL-12 p70, IL-23, IFN-gamma, IL-4, IL-6, IL-17/IL-17A, and TNF-alpha.

Data Representation and Statistical Analysis:

The statistical analysis and data representation was performed using GraphPad Prism 9.0 and FlowJo XV unless otherwise stated. The antibody responses were compared using the RM one-way ANOVA Tukey's Multiple Comparison Test. The cytokine and T cell response against each variant versus wildtype and at different stages of acute infection was calculated and compared using the Wilcoxon matched-pairs signed-rank test. T cell responses were calculated as background-subtracted data by subtracting the values obtained from the SARS-CoV-2 peptide pool stimulation from the DMSO stimulation. Negative values were set to the LOD. The cytokine secretion response upon peptide or TLR stimulation was calculated as fold change data for the correlation analysis by dividing the stimulated wells by unstimulated wells of the same sample. The correlation between the innate and adaptive immune response was performed

using the Pearson correlation test. For metabolomic analysis, processing the raw data by removing drugs and exposome metabolites led to identification of 176 metabolites at all three stages (Visit 1, Visit 3, and Healthy Control). All the statistical and functional analysis, including the PCA, heat map, pathway enrichment analysis, PLS-DA, analysis of variance (ANOVA), was done based on the observed peaks intensity using the online open-source software Metaboanalyst 5.0. Before analysis, a data integrity check was performed, and the raw data were normalized by sum, log-transformed, and scaled by Pareto scaling. The volcano plots were constructed using the online available package VolcanoR (44).

A broadscale Pearson correlation analysis of the metabolites belonging to the V1 and V3 groups with the innate and adaptive immune responses of V1 and V3 was performed. Those metabolites belonging to V1 and V3 that significantly correlated ($p < 0.05$, $r > 0.5$) with the proinflammatory adaptive immune responses and/or TH1 skewed T cell immune responses and has pathway library of KEGG were selected for Pathway Analysis using the Metaboanalyst 5.0 software (45).

Acknowledgment:

We acknowledge the funding through the Mission COVID Suraksha grant (BT/CS0010/CS/02/20) – from BIRAC, Department of Biotechnology, for enabling this study. We thank all the volunteers who donated their blood samples for this study. We sincerely thank the staff and students of the Translational Health Science and Technology Institute (THSTI; Faridabad, India) for helping to ensure the smooth conduct of the study.

Author contributions:

Conceptualization: AA, DR, AB

Methodology: AB, AZ, JD, YK, SG, SM, MT, UM, TS

Investigation: AA, DR, SM, YK, TS, AP

Visualization: AB

Funding acquisition: AA, DR, AB

Project administration: AA, DR, AP

Supervision: AA, DR

Writing – original draft: AB, AZ, AA

Data Analysis: AB, DR, JD, SG, YK, SM, AZ

Writing – review & editing: AA

Competing interests: Authors declare that they have no competing interests.

REFERENCE

1. D. S. Stephens, M. J. McElrath, COVID-19 and the Path to Immunity. *JAMA* **324**, 1279-1281 (2020).
2. N. Sherina *et al.*, Persistence of SARS-CoV-2-specific B and T cell responses in convalescent COVID-19 patients 6-8 months after the infection. *Med (New York, N.Y.)* **2**, 281-295.e284 (2021).
3. A. Grifoni *et al.*, SARS-CoV-2 human T cell epitopes: Adaptive immune response against COVID-19. *Cell host & microbe* **29**, 1076-1092 (2021).
4. N. Le Bert *et al.*, SARS-CoV-2-specific T cell immunity in cases of COVID-19 and SARS, and uninfected controls. *Nature* **584**, 457-462 (2020).
5. J. L. Schultze, A. C. Aschenbrenner, COVID-19 and the human innate immune system. *Cell* **184**, 1671-1692 (2021).
6. D. Mathew *et al.*, Deep immune profiling of COVID-19 patients reveals distinct immunotypes with therapeutic implications. *Science* **369**, eabc8511 (2020).
7. S. Bülow Anderberg *et al.*, Increased levels of plasma cytokines and correlations to organ failure and 30-day mortality in critically ill Covid-19 patients. *Cytokine* **138**, 155389 (2021).
8. M. Secchi *et al.*, COVID-19 survival associates with the immunoglobulin response to the SARS-CoV-2 spike receptor binding domain. *The Journal of Clinical Investigation* **130**, 6366-6378 (2020).
9. C. Rydyznski Moderbacher *et al.*, Antigen-Specific Adaptive Immunity to SARS-CoV-2 in Acute COVID-19 and Associations with Age and Disease Severity. *Cell* **183**, 996-1012.e1019 (2020).
10. P. S. Arunachalam *et al.*, Systems biological assessment of immunity to mild versus severe COVID-19 infection in humans. *Science* **369**, 1210-1220 (2020).

11. Y. Li *et al.*, SARS-CoV-2 induces double-stranded RNA-mediated innate immune responses in respiratory epithelial-derived cells and cardiomyocytes. *Proceedings of the National Academy of Sciences* **118**, e2022643118 (2021).
12. N. Xiao *et al.*, Integrated cytokine and metabolite analysis reveals immunometabolic reprogramming in COVID-19 patients with therapeutic implications. *Nature Communications* **12**, 1618 (2021).
13. B. Isho *et al.*, Persistence of serum and saliva antibody responses to SARS-CoV-2 spike antigens in COVID-19 patients. *Science immunology* **5**, (2020).
14. R. Thiruvengadam, A. Binayke, A. Awasthi, SARS-CoV-2 delta variant: a persistent threat to the effectiveness of vaccines. *The Lancet Infectious Diseases*.
15. U. Sahin *et al.*, COVID-19 vaccine BNT162b1 elicits human antibody and TH1 T cell responses. *Nature* **586**, 594-599 (2020).
16. R. Thiruvengadam *et al.*, Effectiveness of ChAdOx1 nCoV-19 vaccine against SARS-CoV-2 infection during the delta (B.1.617.2) variant surge in India: a test-negative, case-control study and a mechanistic study of post-vaccination immune responses. *The Lancet Infectious Diseases*, (2021).
17. A. Grifoni *et al.*, Targets of T Cell Responses to SARS-CoV-2 Coronavirus in Humans with COVID-19 Disease and Unexposed Individuals. *Cell* **181**, 1489-1501.e1415 (2020).
18. S. S. A. Karim, Q. A. Karim, Omicron SARS-CoV-2 variant: a new chapter in the COVID-19 pandemic. *The Lancet* **398**, 2126-2128 (2021).
19. M. S. Diamond, T.-D. Kanneganti, Innate immunity: the first line of defense against SARS-CoV-2. *Nature Immunology* **23**, 165-176 (2022).
20. A. M. Krieg, J. Vollmer, Toll-like receptors 7, 8, and 9: linking innate immunity to autoimmunity. *Immunological reviews* **220**, 251-269 (2007).

21. M. Sindelar *et al.*, Longitudinal metabolomics of human plasma reveals prognostic markers of COVID-19 disease severity. *Cell Reports Medicine* **2**, 100369 (2021).
22. F.-X. Danlos *et al.*, Metabolomic analyses of COVID-19 patients unravel stage-dependent and prognostic biomarkers. *Cell Death & Disease* **12**, 258 (2021).
23. H. Jia *et al.*, Metabolomic analyses reveals new stage-specific features of the COVID-19. *European Respiratory Journal*, 2100284 (2021).
24. J. C. Páez-Franco *et al.*, Metabolomics analysis reveals a modified amino acid metabolism that correlates with altered oxygen homeostasis in COVID-19 patients. *Scientific Reports* **11**, 6350 (2021).
25. C. del Rio, S. B. Omer, P. N. Malani, Winter of Omicron—The Evolving COVID-19 Pandemic. *JAMA* **327**, 319-320 (2022).
26. L. Ansone *et al.*, Amino Acid Metabolism is Significantly Altered at the Time of Admission in Hospital for Severe COVID-19 Patients: Findings from Longitudinal Targeted Metabolomics Analysis. *Microbiology Spectrum* **9**, e00338-00321 (2021).
27. D. Planas *et al.*, Reduced sensitivity of SARS-CoV-2 variant Delta to antibody neutralization. *Nature* **596**, 276-280 (2021).
28. Y. Gao *et al.*, Ancestral SARS-CoV-2-specific T cells cross-recognize the Omicron variant. *Nature Medicine*, (2022).
29. D. M. Del Valle *et al.*, An inflammatory cytokine signature predicts COVID-19 severity and survival. *Nature Medicine* **26**, 1636-1643 (2020).
30. Z. A. Rizvi *et al.*, Golden Syrian hamster as a model to study cardiovascular complications associated with SARS-CoV-2 infection. *eLife* **11**, e73522 (2022).
31. S. K. Wculek, S. C. Khouili, E. Priego, I. Heras-Murillo, D. Sancho, Metabolic Control of Dendritic Cell Functions: Digesting Information. *Frontiers in Immunology* **10**, (2019).

32. V. Bronte, P. Zanovello, Regulation of immune responses by L-arginine metabolism. *Nature Reviews Immunology* **5**, 641-654 (2005).
33. C. I. Chang, J. C. Liao, L. Kuo, Arginase modulates nitric oxide production in activated macrophages. *The American journal of physiology* **274**, H342-348 (1998).
34. A. Swain *et al.*, Comparative evaluation of itaconate and its derivatives reveals divergent inflammasome and type I interferon regulation in macrophages. *Nature Metabolism* **2**, 594-602 (2020).
35. E. L. Mills *et al.*, Itaconate is an anti-inflammatory metabolite that activates Nrf2 via alkylation of KEAP1. *Nature* **556**, 113-117 (2018).
36. E. H. Kobayashi *et al.*, Nrf2 suppresses macrophage inflammatory response by blocking proinflammatory cytokine transcription. *Nature Communications* **7**, 11624 (2016).
37. J.-W. Song *et al.*, Omics-Driven Systems Interrogation of Metabolic Dysregulation in COVID-19 Pathogenesis. *Cell Metabolism* **32**, 188-202.e185 (2020).
38. J. S. Maras *et al.*, Multi-omics analysis of respiratory specimen characterizes baseline molecular determinants associated with SARS-CoV-2 outcome. *iScience* **24**, 102823 (2021).
39. K. U. Schallreuter, J. W. Wood, A possible mechanism of action for azelaic acid in the human epidermis. *Archives of Dermatological Research* **282**, 168-171 (1990).
40. S. Chaudhuri *et al.*, Comparative evaluation of SARS-CoV-2 IgG assays in India. *Journal of Clinical Virology* **131**, 104609 (2020).
41. J. M. Dan *et al.*, Immunological memory to SARS-CoV-2 assessed for up to 8 months after infection. *Science* **371**, eabf4063 (2021).
42. S. Naz *et al.*, Development of a Liquid Chromatography–High Resolution Mass Spectrometry Metabolomics Method with High Specificity for Metabolite

Identification Using All Ion Fragmentation Acquisition. *Analytical Chemistry* **89**, 7933-7942 (2017).

43. A. Kumar *et al.*, Metabolomic analysis of primary human skeletal muscle cells during myogenic progression. *Scientific Reports* **10**, 11824 (2020).
44. J. Goedhart, M. S. Luijsterburg, VolcaNoseR is a web app for creating, exploring, labeling and sharing volcano plots. *Scientific Reports* **10**, 20560 (2020).
45. J. Chong *et al.*, MetaboAnalyst 4.0: towards more transparent and integrative metabolomics analysis. *Nucleic acids research* **46**, W486-W494 (2018).

FIGURES AND FIGURE LEGENDS

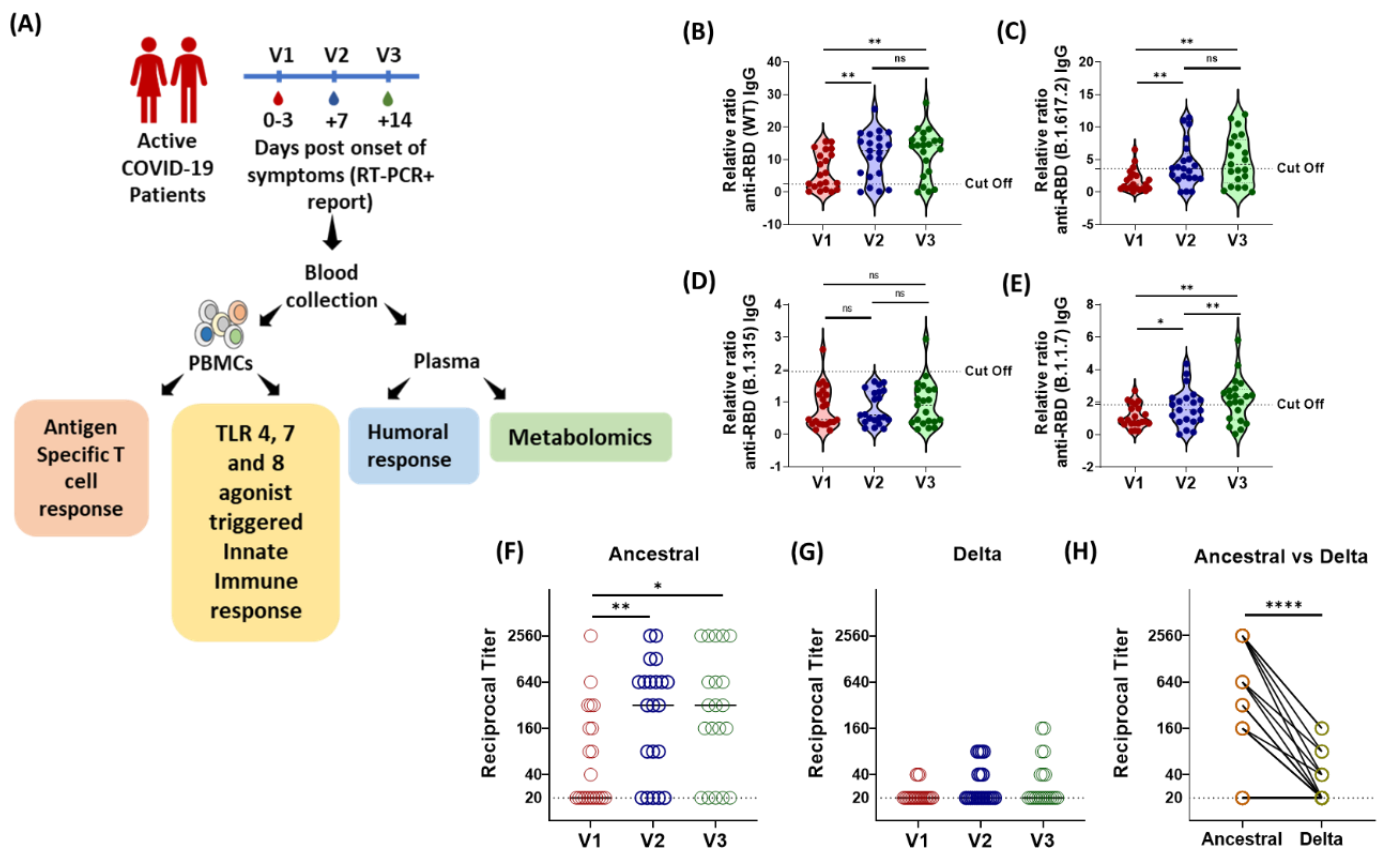


Fig 1: Longitudinal Analysis of Humoral Immune Response against the SARS-CoV-2

during acute COVID-19 infection. (A) Schematic experimental design and longitudinal sample collection at specific time intervals after confirmed SARS-CoV-2 infection in mildly infected patients. (B-E) The longitudinal anti-RBD IgG responses were evaluated by performing ELISA against the RBD proteins of (B) WT (Wuhan isolate) (C) Delta (B.1.617.2) (D) Beta (B.1.315) (E) Alpha (B.1.1.7). All data, represented as ratio-converted ELISA reads to a pool of pre-pandemic negative control samples (relative ratio), were plotted using violin plots.

(F-H) The longitudinal neutralizing antibody titers against (F) the ancestral strain and (G) the delta strain of SARS-CoV-2 during V1 (day 0-3), V2 (day 7) and V3 (day 14) from COVID-19 positivity (H) The paired representation of NAb titers in the active COVID-19 patients during V3 against the ancestral and delta variants of SARS-CoV-2.

The dots represent each individual sample. Tukey's multiple comparisons and two-sided Wilcoxon Signed Rank tests were employed for unpaired and paired analysis, respectively. n.s = not significant, * = $p \leq 0.05$, ** = $p \leq 0.01$, **** = $p < 0.0001$.

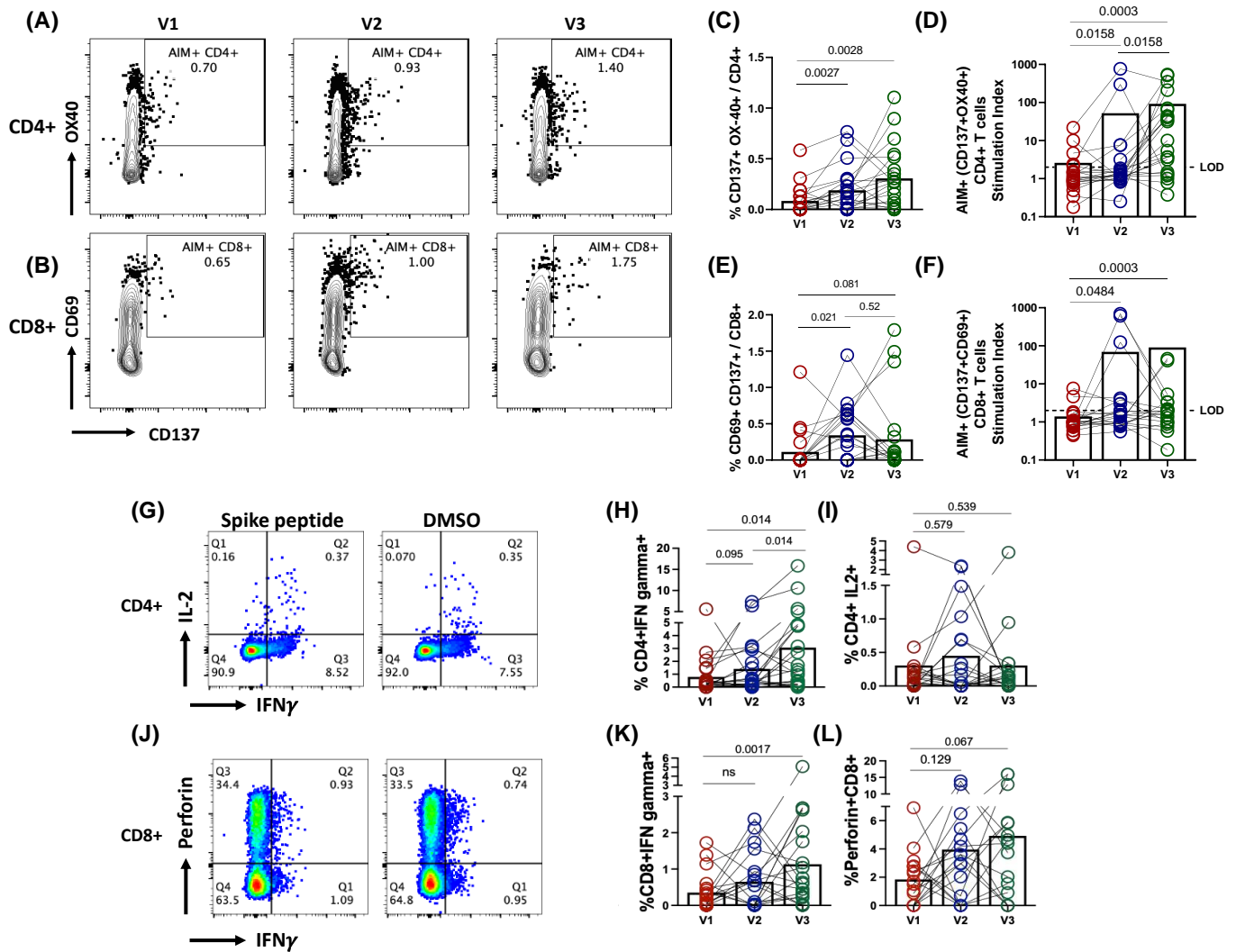


Fig. 2. Longitudinal dynamics of antigen-specific T cell immune responses during COVID-19 infection. Representative flow cytometry plots of SARS-CoV-2 Spike specific T cells expressing activation-induced markers (AIM) (A) CD4+ (CD137+OX40+) (B) CD8+ (CD137+CD69+); (C-F) Longitudinal analysis of the AIM response in paired samples from the same subject (C) percentage frequency of CD4+AIM+ cells (D) Stimulation index (SI) of CD4+ AIM+ cells (E) %frequency of CD8+AIM+ cells (F) SI of CD8+ AIM+ cells.

(G, J) Representative flow cytometry plots for the intracellular cytokine staining (ICS) assay of cells upon stimulation with spike peptide pool compared to the DMSO; Longitudinal analysis of the frequency (percentage of total CD4+ or CD8+ cells) of cytokine+ cells in paired samples from the same subject. (H) CD4+ Interferon gamma (IFN γ) (I) CD4+ Interleukin 2

(K) CD8+ Interferon gamma **(L)** CD8+ Perforin; Each datapoint shown is background subtracted, and bars represent mean values for each time point. Two-sided Wilcoxon Signed Rank tests were employed for paired analysis. LOD = Limit of detection for AIM assay was $SI < 2$.

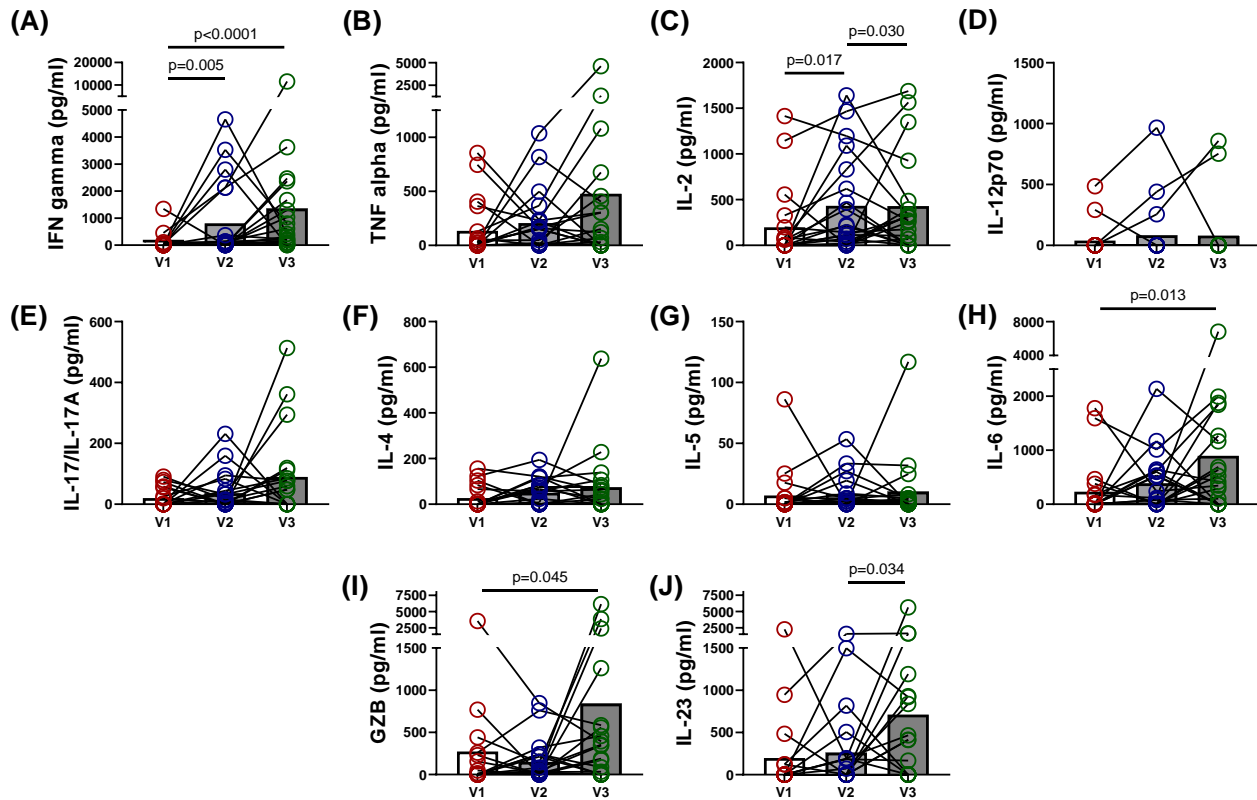


Fig. 3. Longitudinal dynamics of antigen-specific cytokine release by PBMCs during COVID-19 infection. Graphs represent longitudinal cytokine released by paired PBMC samples from the same subject upon stimulation with SARS-CoV-2 spike peptide pool for 18-20h. Each dot represents an individual sample, and the paired samples were analyzed using the two-sided Wilcoxon Signed Rank test. Bars represent mean values.

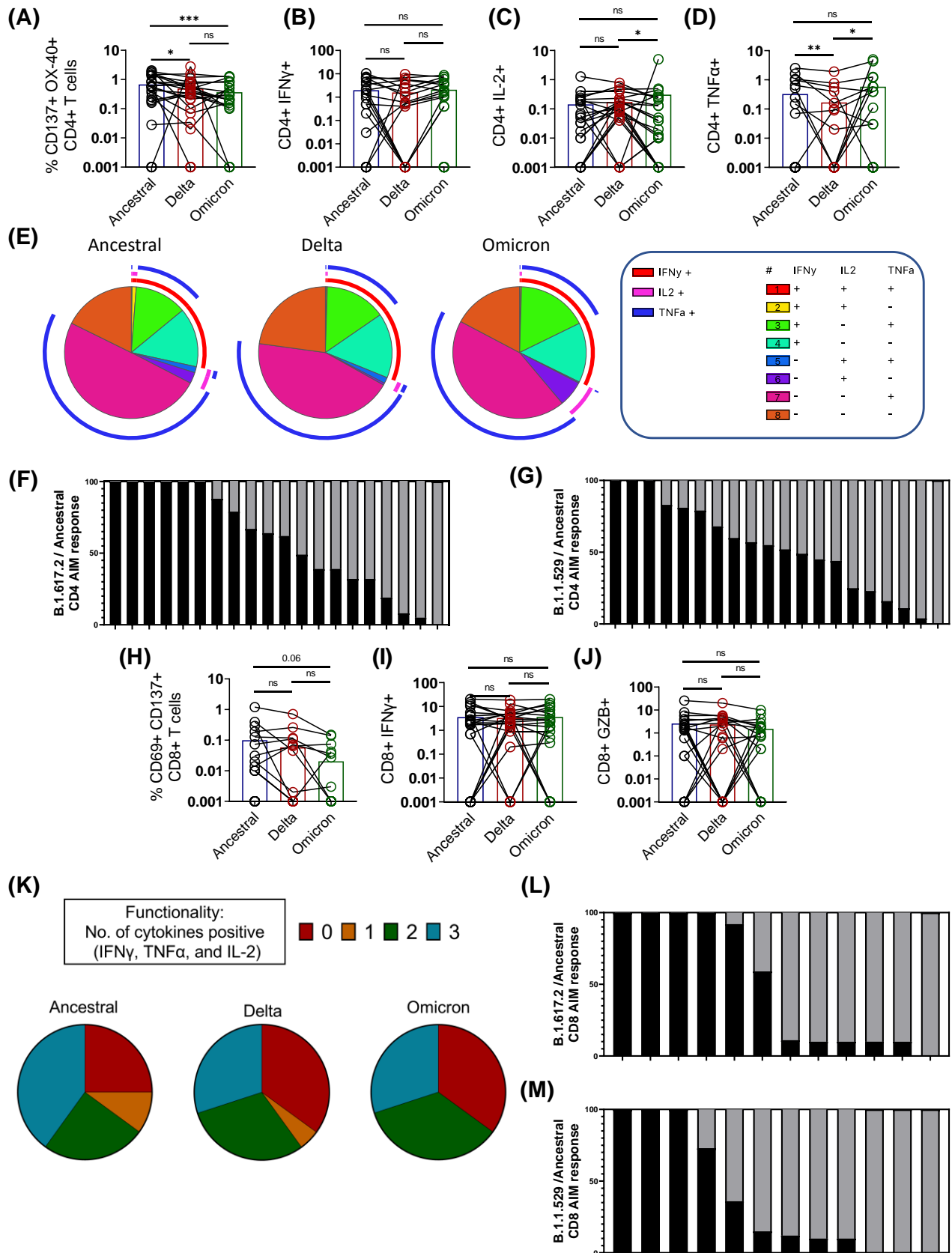


Fig. 4. Cross-reactive CD4+ and CD8+ T cell response against Delta and Omicron Spike

in acute COVID-19 patients. Spike-specific T cell responses in selected samples of active COVID-19 patients (n=24) were simultaneously tested for reactivity against spike peptide pools of WT (Ancestral), Delta (B.1.617.2), and Omicron (B.1.1.529). **(A-D)** Frequencies of antigen-specific CD4+ T cell responses **(A)** CD4+ AIM [CD137+OX40+] **(B)** CD4+ IFN γ **(C)** CD4+ IL2 **(D)** CD4+ TNF α . **(E)** Pie charts showing the mean frequency for each combination of functional profiles of AIM+ CD4 T cell responses in active COVID-19 individuals; Cross-reactive CD4 AIM responses described on a singular basis as **(F)** percentage B.1.617.2/wild-type **(G)** percentage B.1.1.529/wildtype.

(H-J) Frequencies of antigen-specific CD8+ T cell responses **(H)** CD8+ AIM [CD137+CD69+] **(I)** CD8+ IFN γ **(J)** CD8+Granzyme B **(K)** Poly-functional response calculated for an individual sample that is positive for the number of antigen-specific cytokine functions detected;

Cross-reactive CD8 AIM responses described on a singular basis as **(L)** percentage B.1.617.2/wild-type **(M)** percentage B.1.1.529/wildtype.

Bars represent mean values, each dot represents an individual sample, and the solid line connects the same sample stimulated with different peptide pools. AIM, activation-induced markers; GZB, granzyme B; ns, non-significant

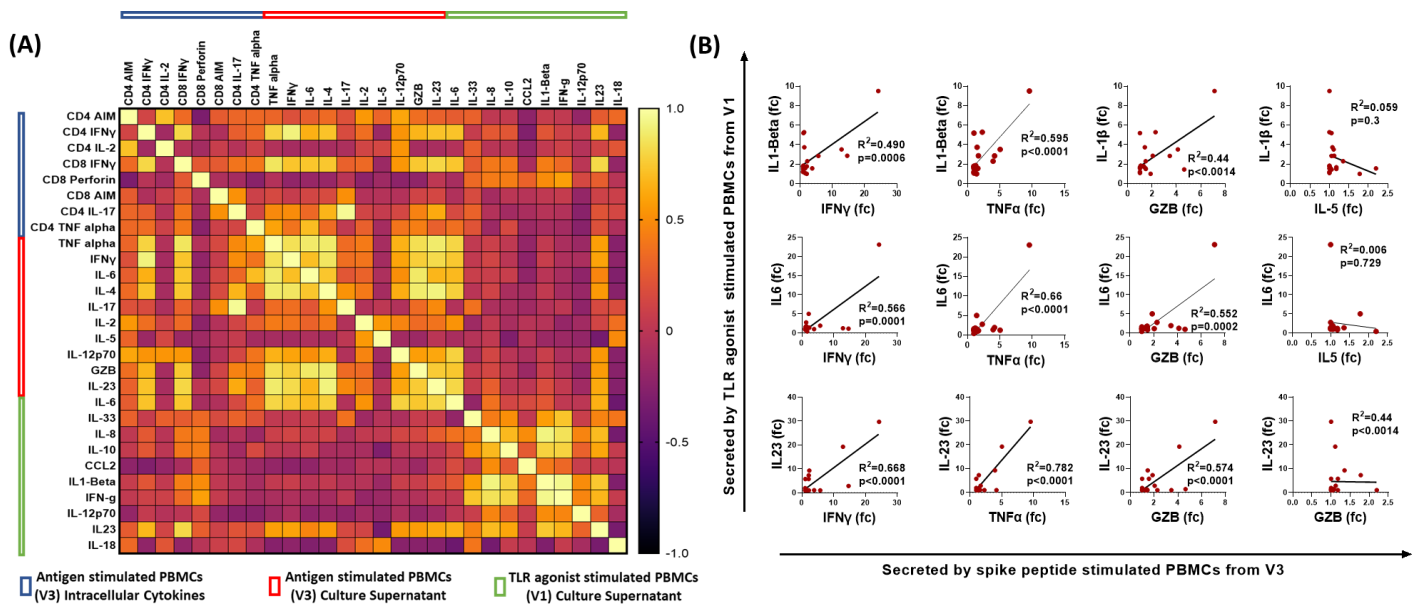


Fig.5. Correlation of early innate immune responses with adaptive immune responses in active COVID-19 patients. Correlation between the cytokine released upon TLR agonist stimulation of PBMCs from early stages of COVID-19 infection (V1) and the magnitude of antigen-specific T cell responses during the later stages of COVID-19 disease (V3). The responses were calculated as fold change in the stimulated wells compared to the unstimulated wells **(A)** A heatmap of correlation analysis; the blue rectangle depicts the analysis of stimulated PBMCs using flow cytometry; the red rectangle represents the fold change of cytokines released in the culture supernatant upon peptide stimulation; and the green rectangle represents the fold change of cytokines released in the culture supernatant upon stimulation with TLR agonists: poly I:C (25 μ g/ml) and R848 (4 μ g/ml) for 24h. **(B)** XY correlation plots where the y axis represents the fold change of cytokines secreted upon TLR agonist stimulation of PBMCs from V1 and the x-axis represents the fold change of cytokines secreted upon peptide pool stimulation of PBMCs from V3. Pearson correlation coefficient is indicated. fc, fold change; GZB, granzyme B

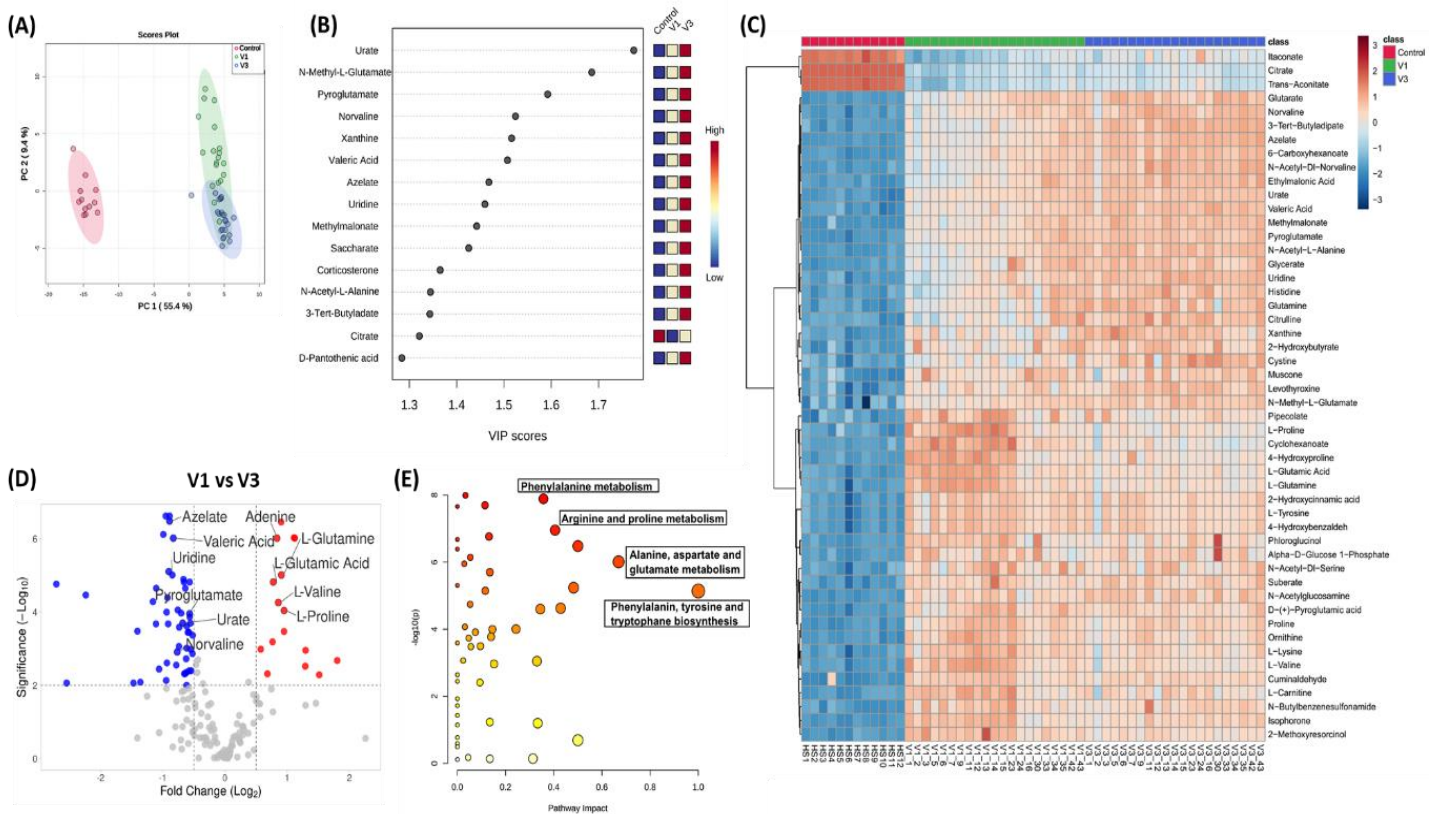


Fig 6. Metabolomic analysis of SARS-CoV-2 patient plasma samples compared to age-matched healthy controls. (A) Principal Component Analysis of the untargeted metabolites of the three groups **(B)** Important features identified by PLS-DA. The colored boxes indicate relative concentrations of designated metabolites in each study group. **(C)** hierarchical cluster analysis is shown as a heatmap of top 50 metabolites (FDR<0.05) **(D)** Pathway enrichment analysis using KEGG of all the metabolites (n=158) that are significantly altered during COVID-19 infection. **(E)** Volcano plot comparing the significantly changed (p=0.001, FC>1.5) metabolites during the early (V1) and later stages of disease (V3).

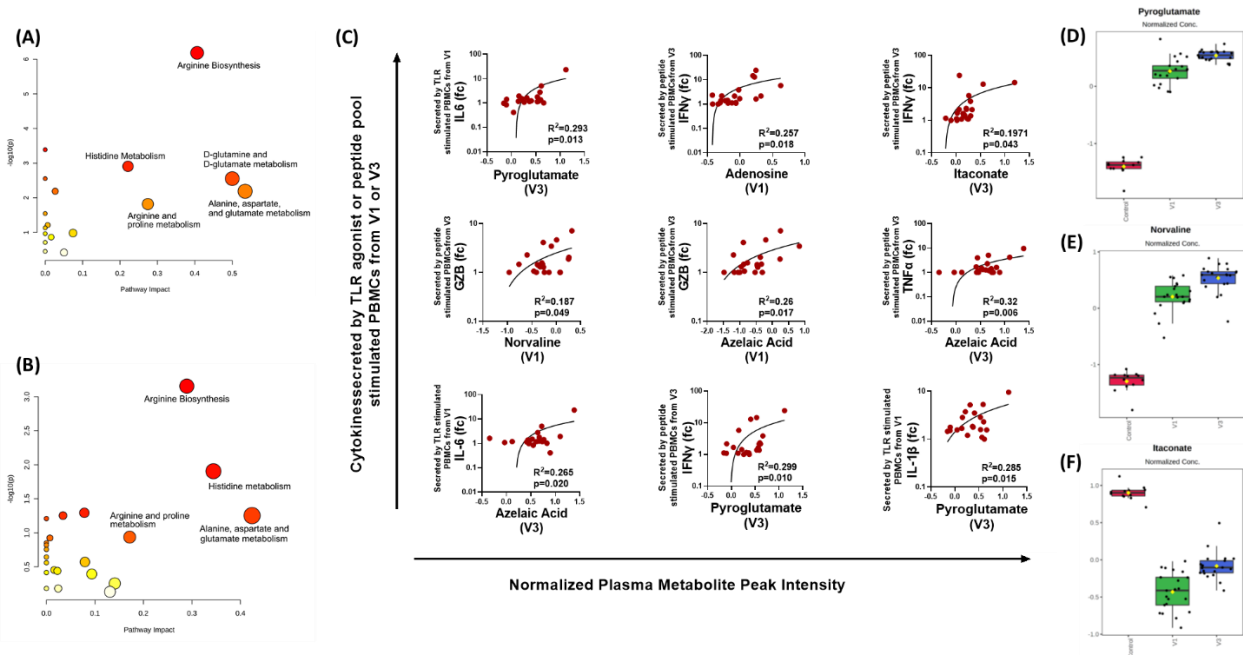


Fig. 7. Correlation of metabolites with immune responses. Pathway analysis of plasma metabolites that significantly correlated ($r > 0.5$, $p < 0.05$) with (A) the innate immune response (V1) and (B) the T cell immune response (V3) (C) Representative correlation plots of metabolites from V1 and V3 that correlate with the cytokine release responses from TLR stimulated innate, and peptide pool stimulated adaptive immune responses. (D-F) Normalized concentrations of metabolites at the three-time points (D) Pyroglutamate (E) Norvaline (F) Itaconate. Each dot represents an individual sample. The bold black line represents the median values. The box represents the interquartile range. The vertical line represents the range of normalized values of the peak intensities of the metabolites estimated by mass spectrometry. Pearson correlation coefficient is indicated. GZB, granzyme B